Spatial and temporal variability of ^{7}Be and ^{210}Pb wet deposition during four successive monsoon storms in a catchment of northern Laos

E. Gourdin, O. Evrard, S. Huon, J.-L. Reyss, O. O. Ribolzi, Thierry Bariac, O. Sengtaheuanghoung, Sophie Ayrault

▶ **To cite this version:**

E. Gourdin, O. Evrard, S. Huon, J.-L. Reyss, O. O. Ribolzi, et al.. Spatial and temporal variability of ^{7}Be and ^{210}Pb wet deposition during four successive monsoon storms in a catchment of northern Laos. Journal of Environmental Radioactivity, 2014, 136, pp.195-205. 10.1016/j.jenvrad.2014.06.008 . cea-02610596

HAL Id: cea-02610596
https://cea.hal.science/cea-02610596

Submitted on 18 May 2020

HAL is a multi-disciplinary open access archive for the deposit and dissemination of scientific research documents, whether they are published or not. The documents may come from teaching and research institutions in France or abroad, or from public or private research centers.

L'archive ouverte pluridisciplinaire **HAL**, est destinée au dépôt et à la diffusion de documents scientifiques de niveau recherche, publiés ou non, émanant des établissements d'enseignement et de recherche français ou étrangers, des laboratoires publics ou privés.

Title

Spatial and temporal variability of ^{7}Be and ^{210}Pb wet deposition during four successive monsoon storms in a catchment of northern Laos.

Authors

Gourdin E. [a], Evrard O. [a], Huon S. [b], Reyss J.-L. [a], Ribolzi O. [c], Bariac T. [d], Sengtaheuanghoung O. [e], Ayrault S. [a]

[a] Laboratoire des Sciences du Climat et de l'Environnement (LSCE), UMR 8212 (CEA-CNRS-UVSQ/IPSL), Domaine du CNRS, avenue de la Terrasse, 91198 Gif-sur-Yvette Cedex, France

[b] Université Pierre et Marie Curie (UPMC), UMR 7618 Bioemco, Case 120, 4 Place Jussieu, 75252 Paris Cedex 05, France

[c] Géosciences Environnement Toulouse (GET), UMR 5563 (CNRS, UPS, IRD), 14 Avenue Edouard Belin, 31400 Toulouse, France

[d] CNRS, UMR 7618 Bioemco, Campus INRA e AgroParisTech, Bâtiment EGER, 78550 Thiverval-Grignon, France

[e] National Agriculture and Forestry Research Institute (NAFRI), P.O. Box 4199, Ban Nogviengkham, Xaythany District, Vientiane, Lao People's Democratic Republic

doi: http://dx.doi.org/10.1016/j.jenvrad.2014.06.008

Abstract

Fallout radionuclides ^{7}Be and ^{210}Pb have been identified as potentially relevant temporal tracers for studying soil particles dynamics (surface vs. subsurface sources contribution; remobilization of in-channel sediment) during erosive events in river catchments. An increasing number of studies compared ^{7}Be: ^{210}Pb activity ratio in sediment and rainwater to estimate percentages of freshly eroded particles. However, the lack of data regarding the spatial and temporal variability of radionuclide wet deposition during individual storms has been identified as one of the main gaps in these estimates. In order to determine this key parameter, rainwater samples were collected at three stations during four storms that occurred at the beginning of the monsoon (June 2013) in the Houay Xon mountainous catchment in northern Laos. Rainwater ^{7}Be and ^{210}Pb activities measured using very low background Germanium hyperpure detectors ranged from 0.05 to 1.72 Bq L^{-1} and 0.02 to 0.26 Bq L^{-1}, respectively. Water $\delta^{18}O$ were determined on the same samples. Total rainfall amount of the four sampled storms ranged from 4.8 to 26.4 mm (51 mm in total) at the time-fractionated collection point S10. Corresponding cumulative ^{7}Be and ^{210}Pb wet depositions at S10 during the sampling period were 17.6 and 2.9 Bq m^{-2}, respectively. The ^{7}Be: ^{210}Pb activity ratio varied (1) in space from 6 to 9 for daily deposition and (2) in time from 3 to 12 for samples successively collected at S10. Intra-event evolution of rainwater ^{7}Be and ^{210}Pb activities as well as $\delta^{18}O$ highlighted the progressive depletion of local infra-cloud atmosphere radionuclide stock with time (washout) which remains consistent with a Raleigh-type distillation process for water vapor. Intra-storm ratio increasing with time showed the increasing contribution of rainout scavenging. Implications of such variability for soil particle labelling and erosion studies are briefly discussed and recommendations are formulated for the further application of the ^{7}Be: ^{210}Pb ratio method, especially in tropical areas under high erosive pressure.

Keywords: Be-7, Pb-210, rainwater, monsoon storm, wet deposition, local spatial temporal variability

1. Introduction

Monsoon storms can have a dramatic impact in mountainous tropical regions where they trigger intense soil erosion with both on-site and downstream consequences (Sidle et al., 2006; Valentin et al., 2008; Morgan, 2009).

Fallout radionuclides brought by rainwater that sorb quickly onto soil particles may be used to discriminate between sediments with different origin (i.e., surface versus depth) and dynamics (i.e., freshly eroded versus re-suspended material; Matisoff et al., 2005; Mabit et al., 2008). During the last years, an increasing number of studies have used ^{7}Be and ^{210}Pb as tracers of soil particles (Evrard et al., 2010; Liu et al., 2011; Olley et al., 2012). Beryllium-7 (^{7}Be), with a half-life of 53.2 days, is a cosmogenic radionuclide naturally produced by spallation of carbon, oxygen and nitrogen in the atmosphere (Lal et al., 1958; Papastefanou and Ioannidou, 1995). Lead-210 (^{210}Pb), which is produced by decay of atmospheric gaseous radon-222 (^{222}Rn) derived from soil uranium-238 (^{238}U) decay chain, has a longer half-life of 22.3 years. Both radionuclides are mainly removed from the atmosphere by washout (Olsen et al., 1985), and brought to the soil (and leaf) surface by wet deposition (Wallbrink and Murray, 1994; Caillet et al., 2001; McNeary and Baskaran, 2003; Ioannidou and Papastefanou, 2006; Conaway et al., 2013). The contrast between the half-lives of both radionuclides makes them potentially interesting tracers for studying soil particles dynamics during erosive events in river catchments (Dominik et al., 1987; Bonniwell et al., 1999; Matisoff et al., 2002; Evrard et al., 2010; Saari et al., 2010). In the case of tropical regions with seasonal monsoon, the rather short period of ^{7}Be results in the almost total decay of previous rainy season inputs to the soil during the following dry season (Gourdin et al., under review). In contrast, ^{210}Pb stock in soils increases as successive inputs may accumulate on particles during the previous years. As ^{210}Pb is also locally produced by soil ^{238}U decay chain, rainfall inputs are distinguished as unsupported-^{210}Pb ($^{210}Pb_{xs}$). Matisoff et al. (2005) proposed to compare ^{7}Be: $^{210}Pb_{xs}$ activity ratios in sediment and rainwater to estimate percentages of freshly eroded particles (assumed to display ratios close to those measured in rainwater) in total transported sediment.

The reliability of such estimates has been recently questioned (Walling, 2012; Taylor et al., 2013). One of the main concerns results from the lack of data to assess the spatial and temporal variability of

radionuclide wet deposition during individual rainfall events. This variability may be controlled by several parameters including, inter alia, the amount of rainwater, the intensity of rainfall, the elapsed-time since last storm, the origin of the raincloud and its trajectory over continent, the latitude and the elevation of the site, the season and the temporal scale considered. Moreover, Su and Huh (2006) documented that an important parameter controlling the activity of ^{7}Be and ^{210}Pb in aerosols (and their depositional fluxes) is the acidity of rain and cloud water. As the use of fallout radionuclides for the study of erosion and sediment dynamics has been recently applied to a variety of study sites including the Houay Xon catchment (Gourdin et al., under review) in northern Laos, it is important to address concerns regarding atmospheric deposition variability and estimate its impact on particle labelling in both space and time. To the best of our knowledge, very few attempts have been made so far to address this issue (e.g., Wallbrink and Murray, 1994; Huh and Su, 2004; Conaway et al., 2013; Pinto et al., 2013; Renfro et al., 2013) whereas monthly and annual fluxes have been more widely documented around the world (e.g., Narazaki et al., 2003; González-Gómez et al., 2006; Huh et al., 2006; Baskaran, 2011; Bourcier et al., 2011; Pham et al., 2013).

In this study, four successive storms were monitored in June at the beginning of the 2013 rainy season, using a network of rainwater sampling stations embedded in the Houay Xon catchment (22.4 km²; Mekong River tributary) in northern Laos. This paper presents ^{7}Be and ^{210}Pb wet deposition (and related ratio) variability across the catchment during these successive storms. Spatially distributed and temporally fractionating devices were designed in order to determine the evolution of deposition during each storm. In addition to fallout radionuclide activities that were determined in collected rainwater, δ^{18}O measurements were conducted for all samples in order to provide complementary information on precipitation dynamics (Dansgaard, 1953; Dansgaard, 1964; Bleeker et al., 1966; Ingraham and Taylor, 1991; Celle-Jeanton et al., 2001). Rainwater δ^{18}O can also be used for hydrograph separation (e.g., Ribolzi et al., 1996; Ladouche et al., 2001) in complement to sediment tracing procedures and improvement in constraining the various end-members contribution requires intra-storm variation monitoring (e.g., Harris et al., 1995; Klaus and McDonnell, 2013). This overall work also specifically discusses the need to monitor variability in order to better constrain the use of ^{7}Be and ^{210}Pb as tracers of sediment dynamics in tropical areas under high erosive pressure.

2. Materials and methods

2.1. Study site

The Houay Xon (HX) catchment is located south of Luang Prabang (LP) urban area in northern Laos (**Fig. 1**). The HX River is a tributary of the Nam Dong River, flowing into the Mekong River within the city of LP (Ribolzi et al., 2010). The upstream Houay Pano (HP) catchment is part of the MSEC (Monitoring Soil Erosion Consortium) network since 1998 (Valentin et al., 2008). Elevation within the HX catchment ranges between *ca.* 270–1300 m a.s.l.

[Fig. 1]

The region is characterized by a summer monsoon climate. Mean annual cumulative rainfall between 1960 and 2013 amounts to *ca.* 1302 ± 364 mm y^{-1} (Bricquet et al., 2003; Patin et al., 2012). Over 80 % of annual rainfall occurs during the rainy season between May and October (**Fig.1**; Ribolzi et al., 2008). The characteristics of the six rainfall monitoring and/or sampling stations are summarized in **Table 1**.

[Table 1]

Location of each station across the Houay Xon River catchment is shown on **Fig. 1.**

2.2. Sampling and data collection

Rainfall intensity was monitored with six automatic pluviometers and eight cumulative rain gauges (**Fig. 1**). Rainfall samples were collected using both time-integrating and time-fractionating devices. To allow time-fractionated collection of rainwater, a metallic roof with a collecting area of *ca.* 4 m^2 was equipped with a PVC gutter, connected to a succession of tanks (18L each; photographs on **Fig. 2**).

[Fig. 2]

Each tank was equipped with a floating plastic ball of the proper size that prevented rainwater inflow when the tank was full (auto-capping system), allowing filling of the next tank to start without subsequent water mixing between tanks. Subsequent fractionation of rainfall corresponded to *ca.* 4.7 mm per tank. After each rainfall event, rainwater-containing tanks were separated from the collecting device and screw-capped to avoid evaporation during transportation to the field laboratory.

Cumulative rain collectors at S4 and HX3 consisted in 0.14 m² buckets placed in open areas at least 1m above ground level to avoid splash contamination.

2.3. Sample preparation and radionuclide analyses

To reduce the volume of rainwater that is required to conduct direct gamma spectrometry analyses, fallout radionuclide recovery was performed in the field by co-precipitation with aluminium hydroxides (Ciffroy et al., 2003; Evrard et al., 2010; Gourdin et al., in review). Samples were prepared by adding 1.5 g of aluminium chloride hexahydrate. Co-precipitation was achieved by addition of 1N NaOH solution until pH attained 8.5-9.0. After 5 hours, the supernatant was removed and the precipitates were placed in an aluminium tray and dried in an oven. All residues were placed in polypropylene tubes and sealed airtight. Gamma spectrometry analysis was conducted with the low-background, high-efficiency, well-type Ge detector of the Laboratoire Souterrain de Modane (LSM), located under the Fréjus Mount in the French Alps where a protection against cosmic rays is achieved by a 1700 m rock cover (Reyss et al., 1995). Counting time ranged between 1 and 3 days depending on sample activity.

Radionuclide activities were measured in a total of 15 individual rainwater samples. The ^{7}Be and ^{210}Pb activities were determined at 477.6 keV and 46.5 keV, respectively. ^{210}Pb, was calculated by subtracting the supported activity from the total ^{210}Pb activity (measured at 46.5 keV) using two ^{226}Ra daughters, i.e. ^{214}Pb (average count at 295.2 and 351.9 keV) and ^{214}Bi (609.3 keV). All measurements were corrected for background level determined every two months as well as for detector and geometry efficiencies. Activities were also decay corrected to the sampling date. All results were expressed in mBq L^{-1}. Uncertainties on radionuclide activities correspond to 1σ counting statistics.

2.4. Rainwater $\delta^{18}O$ measurements

Rainwater sample aliquots were recovered in 30-mL glass flasks, and filtered with <0.2 µm acetate filters. Stable oxygen isotopes measurements ($\delta^{18}O$) were carried out using the standard CO_2 equilibration method (Epstein and Mayeda, 1953) and determined with a VG Optima® mass spectrometer (IEES-Paris, Thiverval-Grignon, France). Isotopic ratios are reported using the $\delta^{18}O$ notation, relative to the Vienna-

Standard Mean Ocean Water (V-SMOW; Gonfiantini, 1978) with an analytical precision better than ±0.1‰.

3. Results and discussion

3.1. Rainfall characteristics

Between June 2 and June 4, 2013, the total amount of rainfall reached *ca.* 45 ± 10 mm for most monitoring stations, except in the upper part of the catchment - over 600 m a.s.l. - that only received 30 ± 1 mm of cumulative rainfall over 72h (**Table 2**).

[Table 2]

Four storms, referred to as Storm 1 to 4 in the remainder of the text, with total rainfall amount exceeding 5 mm occurred during the study period (**Fig. 3**).

[Fig. 3]

Time lags between rainfall onset at the different stations indicate progressive cloud displacement pathway above the study site. Most clouds observed in the field originated from the west of the catchment (where the valley is wider) and moved towards the northeast. Consequently, all storms were first recorded at S10 and then migrated towards S4, CIM and finally S1. However, somewhat different behaviours were also observed from one storm to the other. During the storm of June 2, rainfall started at S4 after CIM and S1, suggesting that a second cloud triggered rainfall in the upper part of the catchment and converged with the one that moved from S10 over S4. This would also explain the higher maximum rainfall intensity (1.6 mm min^{-1}) recorded at S4 (**Fig. 3**). The storm that occurred overnight on June 4 (01:30) was recorded by all pluviometers within less than 5 min and nearly synchronously at S10 and S4, distant of almost 2.5 km. Furthermore this event was characterized by a low rainfall intensity (*ca.* 0.2 mm min^{-1}; **Fig. 3**). This behaviour suggests that this event was triggered by a different type of precipitation from the other recorded storms, which is also supported by fallout radionuclide and $\delta^{18}O$ data (see 3.2 and 3.3). Small storms occurred locally at S10 on June 2 in the morning and at upper stations on June 4 in the evening (**Fig. 3**).

3.2. Rainwater $\delta^{18}O$ evolution

Fractionated sampling at S10 produced 6 successive samples on June 2 and 6 samples on June 4. Detailed evolution of rainfall intensity at S10 associated with each collected rainwater sample is provided on **Fig. 4**.

[Fig. 4]

Collected rainwater oxygen-18 isotopic enrichment ($\delta^{18}O$) ranged between -9.9 and -6.4 ‰.

During storms 1 and 2, values ranged between -8.5 and -6.4‰ whereas they varied between -9.9 and -8.5‰ during storms 3 and 4. This behaviour suggests differences in the isotopic composition of the related air masses. Dansgaard (1964) reported monthly rainfall $\delta^{18}O$ in Luang Prabang from -13 to 0‰ significantly correlated with the amount of precipitation, as also mentioned by Araguas-Araguas et al. (1998; $r^2 = 0.55$). In both studies, no dependence of $\delta^{18}O$ to the temperature effect was put forward. The mean $\delta^{18}O$ of rainwater during the rainy season (from May to September) reported by Araguas-Araguas et al. (1998) was -8.3‰, whereas it was -4.3‰ during the dry season (from October to April). This difference reflects the increased previous depletion of air masses in heavy isotopes during rainy season before they reached Luang Prabang. This depletion is due to the successive storms occurring during vapor travel from its source, i.e. mainly Indian Ocean in June according to low altitude (850 hPa) atmospheric circulation models (Wang et al., 2003; Vuille et al., 2005) that report low-level westerlies. This process likely explains the depleted $\delta^{18}O$ values found for storms 3 and 4. At regional scale, precipitation $\delta^{18}O$ has been shown to be negatively correlated with monsoon strength (Vuille et al., 2005), although weak or insignificant relationships were found at individual stations likely due to rather short record length. As shown on **Fig. 4**, rainwater $\delta^{18}O$ displayed temporal decreasing patterns for each storm (up to -2 ‰ for 10 mm cumulative rainfall depth between samples L1S10A and L1S10C). This behaviour is consistent with Rayleigh-type distillation processes (Dansgaard, 1964). However, at the end of storm 1, on June 2, an increase of $\delta^{18}O$ was observed as rainfall intensity progressively decreased. This could be the consequence of either rainfall intensity decrease (the so called “amount effect” in Dansgaard, 1964) and/or vertical mixing with another rainfall enriched in ^{18}O. Fractionation by evaporation of rain drops

during rainfall is another possible explanation. Such increases of $\delta^{18}O$ after rainfall intensity peak were reported by e.g. Dansgaard (1953), Bleeker et al. (1966) and Celle-Jeanton et al. (2001) for different types of precipitation events. As suggested by the latter, this re-increase trend could result from the decrease of raindrop formation altitude (maximum at rainfall intensity peak).

3.3. Temporal variability of radionuclide activity in rainwater

Rainwater ^{7}Be and ^{210}Pb activities ranged 174-640 ± 8 mBq L^{-1} and 15-137 ± 2 mBq L^{-1}, respectively (**Fig. 4; Appendix**). Variations in ^{210}Pb activity were larger for the June 2 event (30-137 ± 2 mBq L^{-1}) than on June 4 (15-72 ± 1 mBq L^{-1}). This observation is also valid for ^{7}Be activity, ranging 255-640 ± 8 mBq L^{-1} on June 2 and also, despite the occurrence of three distinct storms (**Fig. 4**), ranging 174-342 ± 5 mBq L^{-1} on June 4 (**Appendix**).

On June 2, the first sample collected at S10 (L1S10A; **Fig. 4**) corresponded to the mixing rainwater of an early event (2.4 mm; 10 min) that occurred at *ca.* 11:00 a.m. and of the first 2 mm of rainfall of the afternoon. This sample corresponds to the highest ^{7}Be and ^{210}Pb activities recorded at this station throughout the studied period. The five following samples (L1S10B to L1S10F) are progressively depleted both in ^{7}Be and ^{210}Pb with time (**Fig. 4**). Similar observations were previously made in different environments around the world (e.g., Wallbrink and Murray, 1994; Ishikawa et al., 1995). The first millimetres of rainfall showed higher concentrations in fallout radionuclides and these activities decreased as ^{7}Be and ^{210}Pb were progressively removed from the atmosphere and/or the raincloud by rainfall. For the June 2 storm, well-defined negative exponential relationships can be drawn for both ^{7}Be and ^{210}Pb activities (in Bq L^{-1}) versus cumulative rainfall (**Fig. 5a**).

[Fig. 5]

Similarly, Ishikawa et al. (1995) reported a negative exponential relationship ($C_{(t)} = a * e^{-k*t} + b$) between rainwater radionuclide concentrations ($C_{(t)}$) and the time elapsed since the beginning of rainfall (t). They assigned to a and b the respective concentrations of washout (a) and rainout (b). Positive and statistically meaningful logarithmic correlations can also be established between cumulative wet deposition of both radionuclides and cumulative rainfall (**Fig. 5c**). Total wet deposition of ^{7}Be on June 2 event amounted to

11.6 Bq m^{-2} (**Fig. 5c; Table 3**) remaining in the same order of magnitude than the mean supply of 13.4 Bq m^{-2} (range: 0.03 – 108 Bq m^{-2}) reported by Wallbrink and Murray (1994) in southern Australia from individual rainfall events, although direct comparison is excluded as climate and latitude of both study areas are very different. Total ^{210}Pb wet deposition on June 2 reached 1.9 Bq m^{-2} d^{-1} which remains in the range of values 0.2 - 4.7 Bq m^{-2} d^{-1} reported by McNeary and Baskaran (2003) in Detroit (USA).

The last sample (L1S10F) collected on June 2 showed an increasing ^{7}Be activity that may result from the additional contribution of a second small cloud, also suggested by the observed δ^{18}O increase (**Fig. 4**).

In addition to the depletion of both radionuclides in rainwater during the storm, a two-fold increase in their ^{7}Be: ^{210}Pb activity ratio was observed, from 4.7 ± 0.1 to 10.4 ± 0.7 (**Fig. 4; Appendix**), due to the fact that ^{210}Pb deposition decreased proportionally more than ^{7}Be deposition. The difference in the vertical distributions of both radionuclides (e.g., Moore et al., 1973; Talpos and Cuculeanu, 1997) that results from their contrasted origins (i.e., upper atmosphere for ^{7}Be, and ground level ^{222}Rn emission for ^{210}Pb) could explain this behaviour. Moreover, the shift of ^{7}Be: ^{210}Pb ratio outlines the progressive depletion of below-raincloud atmospheric radionuclide stock by washout, whereas the contribution of rainout to total scavenging (washout + rainout) increased.

On June 4 (**Fig. 4 and 5**), the three successive storms (referred to as storms 2, 3 and 4) amounted to 4.7 mm (L2S10G), 11.1 mm (L2S10H - I - J) and 8.6 mm (L2S10K - L) respectively. Compared to the second storm, the first one showed a rather similar ^{7}Be activity but a higher ^{210}Pb activity, which resulted in a very low ratio (3.1; **Fig. 4 and 5**). The two subsequent storms 3 and 4 presented behaviours similar to the one observed on June 2, namely a decrease in both radionuclide activities and an increase of the rainwater ^{7}Be: ^{210}Pb ratio that varied between 4.7 and 11.7 (**Fig. 4; Appendix**).

The temporal variability of radionuclide deposition from one storm to the next at S10 is shown in **Fig. 6**. The ^{7}Be deposition seems to be mainly related to total rainfall amount, whereas ^{210}Pb displays a rather different behaviour. The ^{210}Pb deposition triggered by the three storms that occurred on June 4 is quite similar despite their contrasted amounts of precipitation. However, the global ^{7}Be: ^{210}Pb ratio associated with each storm highlights the particularity of storm 2 during which this ratio was almost twice smaller (**Fig. 6**).

[Fig. 6]

Storm 2 was furthermore characterized by the lowest rainfall intensity (4.7 mm in 48 min) and the highest mean $\delta^{18}O$ (-7.2‰; **Fig. 4**; **Appendix**). The high concentration of ^{210}Pb observed for storm 2 may also be connected with the length of the preceding dry period (1.4 day) compared with the ones of the following storms, 0.5 and 0.1 days for storm 3 and storm 4, respectively.

The magnitude of radionuclide deposition temporal variability observed are different whether intra-storm and inter-storms variations are taken into account (**Fig. 4-5; Appendix**). The activity ratio of rainwater collected at S10 has also varied with time, from 3.0 to 12.4 with a mean value of 6.0 for total wet deposition. The values for total depositions from one storm to the next were less contrasted than variations between individual samples as they correspond to average ratios ranging 3.1 - 7.2 (**Fig. 6**). The implications of this variability for sediment tracing are discussed in section 3.5.

Although a limited number of samples was collected in this study, our results show that the ^{18}O-depletion of rainwater follows that determined for ^{7}Be and ^{210}Pb until rainfall reaches its maximum intensity. Therefore at local scale the Rayleigh type distillation process, responsible for $^{18}O/^{16}O$ partition between water vapour and liquid phases during precipitation, is consistent with upper atmosphere ^{7}Be scavenging and below-cloud ^{210}Pb washout. This trend displays discrepancies when rainfall intensity decreases, indicating that other processes such as raindrop evaporation for $\delta^{18}O$ are operating as mentioned in section 3.2.

3.4. Spatial variability of radionuclide wet deposition

In addition to time-fractionating sampling at S10, one cumulative sample was collected at S4 for each rainy day and at HX3 for June 2 only (**Tables 1 and 3**). Based on the characteristics of the station described in **Table 1**, radionuclide activities in rainwater (ranges: 0.17-1.72 Bq L^{-1} and 0.02-0.26 Bq L^{-1} for ^{7}Be and ^{210}Pb respectively) were converted into cumulative wet deposition (in Bq m^{-2}) for each sample or station (**Table 3**). The total deposition estimates for each collection point are displayed in **Table 3**.

[Table 3]

On June 2, ^{7}Be and ^{210}Pb wet deposition ranged 11.6 - 46.6 ± 2 Bq m^{-2} and 1.9 - 7.1 ± 0.3 Bq m^{-2}, respectively. Despite large variations in ^{7}Be and ^{210}Pb activity, stations HX3, S10 and S4 presented very similar ratios of *ca.* 6. Spatial variability of wet deposition ratio was therefore rather low (11% including analytical uncertainty) during the storm.

Estimates of wet deposition for June 4 could only be obtained for S10 and S4 (**Table 3**). Despite an almost two-fold higher amount of rainfall for June 4 at S4 (39.8 mm; **Table 2**), ^{210}Pb deposition values were rather similar (3.8 ± 0.4 Bq m^{-2}) to the ones documented for June 2. However, ^{7}Be deposition triggered by the succession of storms of June 4 was higher (33.8 ± 2.1 Bq m^{-2}) than for the single-storm June 2 deposition (23.3 ± 0.5 Bq m^{-2}; **Table 2**). The difference between depositions at S10 and S4 were also higher for June 4 than for June 2. Depositions for June 4 at S10 represented only 18% of ^{7}Be and 29% of ^{210}Pb deposition at S4, whereas they represented *ca.* 50% for June 2. The related ^{7}Be: ^{210}Pb ratio at S4 was also higher than for June 2, with 9.0 ± 1.5 vs. 6.0 ± 0.3.

Total wet deposition throughout the study period was obtained by adding June 2 and June 4 deposition values (**Table 3**). Overall, the spatial variability of radionuclide deposition in the catchment was high with differences up to almost 6-fold for ^{7}Be and 4-fold for ^{210}Pb from one station to the next during storm 1. As the succession of rainfalls reduces both intra- and inter-event differences between the collection points, higher variability can be expected at shorter time-scales. The impact of such differences on soil or sediment particles labelling by rainwater radionuclides is not straightforward and is discussed in section 3.5.

3.5. Impact of ^{7}Be and ^{210}Pb wet deposition local variability on soil and sediment activity and ratio

As overland flow loaded with fresh sediment could not be collected during the four studied storms, we do not have direct information on the evolution of particle activity both in time and space across the Houay Xon catchment. We can, nevertheless, make several assumptions on the behaviour of fallout radionuclides by considering rainfall inputs. **Table 4** summarizes radionuclide wet deposition data documented in the literature for individual storm events.

[Table 4]

The comparison of our results with published data is not straightforward as the duration of experiments, the number of measurements and the site characteristics are different from one study to the next. However, several relevant conclusions can be drawn from a cautious comparison. In their study, Renfro et al. (2013) reported cumulative wet depositions for both radionuclides during four individual storms that brought *ca.* 8 - 40 mm of rainfall in New York (USA). The ^{7}Be depositions are higher than those recorded in the Houay Xon catchment in contrast to ^{210}Pb depositions that are lower, resulting in very high ^{7}Be: ^{210}Pb ratios (up to 286 ± 71). Monthly deposition values, although less contrasted, displayed values up to 28.1 ± 0.9. This behaviour is consistent with the coastal location of the study site and similar to global trends observed by Lozano et al. (2013) in the Gulf of Cadiz (SE Spain) where monthly deposition ratios reached 30.6 ± 2.2. Both study report poor ^{210}Pb content in precipitation, consistent with the local marine origin of air masses. In contrast, the Houay Xon River catchment is located several hundreds of km away from the ocean and, as main monsoon atmospheric currents in this region come from the southwest, a minimum 625 km-long travel from the Gulf of Martaban (Wang et al., 2003; Vuille et al., 2005) above the continent is required for water vapor to reach the study site. During their travel, air masses are progressively loaded with ^{222}Rn, and vapor / aerosol ^{210}Pb activity subsequently increases until condensation leads to rainfall (Turekian et al., 1977). This behaviour explains the higher ^{210}Pb activities and lower ^{7}Be: ^{210}Pb ratios observed in our study site.

Although they are difficult to compare with most studies, as they were determined at different spatial scales, our data remain consistent with spatial coefficients of variation of ^{7}Be deposition reported during individual rainfall events by Pinto et al. (2013) and Conaway et al. (2013). However, the sampling techniques employed by the former, who restricted rainwater sampling to the first 5 mm of rainfall, may have artificially increased the heterogeneity between samples for storms totalizing more than 5 mm. The very first fallout radionuclide supply by rainfall is significantly different from the one in total rainwater. We should therefore expect that total rainfall collection would have displayed more homogenous deposition values.

Because of its cumulative behaviour, few studies addressed the spatial variability of inter-storm ^{210}Pb deposition, and most of them focused on monthly to seasonal trends. Compared to depositions in Japan

and Korea reported by Yamamoto et al. (2006), the highest daily depositions observed in the Houay Xon catchment (7.1 ± 0.3 Bq m^{-2}; **Table 3**) are in the range of the lowest ^{210}Pb monthly depositions (~2-8 Bq m^{-2} ; **Table 3**) but represent ~1/30 of the highest monthly deposition values (~245 Bq m^{-2}). Based on the collection of rainwater samples with monthly to daily collection frequencies, Huh et al. (2006), reported similar daily values than in our study for northern Taiwan sites (latitude 25°N comparable to our study site), sampled between 1996 and 2005 (**Table 3**). Furthermore, their two study sites separated by *ca.* 20 km, provided rainwater ^{7}Be: ^{210}Pb ratios with a lower variability (mean: 29%) than radionuclides daily wet deposition (**Table 4**). ^{7}Be and $^{210}Pb_{xs}$ soil inventories were also reported by Huh and Su (2004) for 25 landscape units sampled between 1997 and 2001. The variation coefficient, obtained for samples collected in the same landscape unit, displayed a wider variability (10 - 85% of the mean value, up to *ca.* 5300 Bq m^{-2}) than the ones reported for ^{7}Be by Wallbrink and Murray (1996) in Australian soils (5 - 25% depending on the type of vegetation cover) or by Iurian et al. (2013) in Austria (19%). Furthermore, as previously described, the spatial variability of the deposition ^{7}Be: ^{210}Pb ratio may be rather limited for a single storm whereas it may exceed analytical uncertainties when considering a succession of storm events. From our literature review, we see that reliable estimates of local spatial variability of wet fallout radionuclide deposition at storm / flood temporal scales are not necessarily well documented in most studies, despite the need for taking into account this key parameter.

3.6. Implications for the use of the ^{7}Be: ^{210}Pb ratio method to constrain sediment dynamics

In this context, information on spatial variability of both pre-event soil activities and wet deposition during the storm event appears crucial to estimate the “fresh sediment” signature (Matisoff et al, 2005). As shown in this study, intra-storm temporal variability of radionuclide wet deposition is affected by washout and rainout processes resulting in progressively decreasing concentrations in rainwater. Considering this behaviour, it appears necessary to collect rainfall throughout the entire event to estimate wet deposition levels for each location. However, as this intra-event evolution has already been described in various climatic and geomorphological contexts (e.g. Wallbrink and Murray, 1994; Ishikawa et al, 1995), cumulative rainfall samples may be sufficient to estimate total deposition. Therefore, preference may be

given to increase the number of sampling stations across space rather than to install time-fractionating collection devices.

As described above, wet deposition varies greatly from one storm to the next. It implies that determining the deposition value associated with the storm that triggered a specific flood is necessary. Attributing a constant deposition value to different floods may be irrelevant.

4. Concluding remarks

Based on this experiment and in the aim of improving knowledge on ^{7}Be and ^{210}Pb wet deposition variability and its impact on soil/eroded particles labelling, several recommendations for future studies may be put forward. Rainwater collection should be designed in order to:

- ensure complete rainfall sampling, as partial sampling (e.g. only the first 5 mm, or short-time and non-subsequent collection) will not be representative of the total wet deposition supply and the corresponding soil / sediment labelling (possible 30% underestimation of total deposition ratio);

- separate the respective depositions of successive storms, since the last erosive flood, as particle-labelling may evolve from one storm to the next;

- ensure spatially distributed collection of cumulative rainwater at the storm scale as spatial variability of wet deposition may be very different for each storm;

- reduce as much as possible the uncertainties on cumulative rainfall amounts by preventing potential water evaporation during sample collection (particularly in tropical environments);

The results of this study also demonstrated the interest of providing additional complementary data, in particular water stable isotopes, to document the precipitation-related air masses history. Temporal high-resolution monitoring of storm events is required to discriminate rainwater from soil pre-existing water contributions for hydrograph separation procedures using water stable isotopes as well as for ^{7}Be – ^{210}Pb labeling and monitoring experiments for sediment dynamics budgets.

Acknowledgements

The authors would like to thank the Lao NAFRI (National Agriculture and Forestry Research Institute in Vientiane) and the MSEC project (Multi-Scale Environment Changes) for their support. They are also grateful to Keo Oudone Latsachack, Bounsamai Soulileuth, Chanthamousone Thammahacksa and Thierry Henry des Tureaux for their kind, constant and irreplaceable help in the field. Thanks to Patricia Richard (IEES-Paris, Thiverval Grignon, France) for oxygen-18 analysis of water. EG received a PhD fellowship from Paris-Sud University. This work received financial support from the French CNRS EC2CO / BIOHEFECT program (Belkong project). Finally, the authors would like to thank two anonymous reviewers, whose comments helped to improve a former version of the manuscript.

References

Araguas-Araguas, L., Froehlich, K., Rozanski, K., 1998. Stable isotope composition of precipitation over southeast Asia. J. Geophys. Res. 103, 28721–28742.

Baskaran, M., 2011. Po-210 and Pb-210 as atmospheric tracers and global atmospheric Pb-210 fallout: a review. J. Environ. Radioact. 102, 500–13.

Bleeker, B.W., Dansgaard, W., Lablans, W.N., 1966. Some remarks on simultaneous measurements of particulate contaminants including radioactivity and isotopic composition of precipitation. Tellus 18, 773–785.

Bonniwell, E.C., Matisoff, G., Whiting, P.J., 1999. Determining the times and distances of particle transit in a mountain stream using fallout radionuclides. Geomorphology 27, 75–92.

Bourcier, L., Masson, O., Laj, P., Pichon, J.M., Paulat, P., Freney, E., Sellegri, K., 2011. Comparative trends and seasonal variation of ^{7}Be, ^{210}Pb and ^{137}Cs at two altitude sites in the central part of France. J. Environ. Radioact. 102, 294–301.

Bricquet, J.-P., Boonsaner, A., Bouahom, B., Toan, T.D., 2003. Statistical Analysis of Long Series Rainfall Data: A Regional Study in South-East Asia, in: Maglinao, A.R., Valentin, C., Penning de Vries, F. (Eds.), From Soil Research to Land and Water Management: Harmonizing People and Nature: Proceedings of the IWMI-ADB Project Annual Meeting and 7th MSEC Assembly. Vientiane (LAO). IWMI-ADB Project Annual Meeting; MSEC Assembly, 7., Vientiane (LAO), pp. 83–89.

Caillet, S., Arpagaus, P., Monna, F., Dominik, J., 2001. Factors controlling ^{7}Be and ^{210}Pb atmospheric deposition as revealed by sampling individual rain events in the region of Geneva, Switzerland. J. Environ. Radioact. 53, 241–56.

Celle-Jeanton, H., Travi, Y., Blavoux, B., 2001. Isotopic typology of the precipitation in the Western Mediterranean Region at three different time scales. Geophys. Res. Lett. 28, 1215–1218.

Ciffroy, P., Reyss, J.L., Siclet, F., 2003. Determination of the residence time of suspended particles in the turbidity maximum of the Loire estuary by ^{7}Be analysis. Estuar. Coast. Shelf Sci. 57, 553–568.

Conaway, C.H., Storlazzi, C.D., Draut, A.E., Swarzenski, P.W., 2013. Short-term variability of ^{7}Be atmospheric deposition and watershed response in a Pacific coastal stream, Monterey Bay, California, USA. J. Environ. Radioact. 120, 94–103.

Dansgaard, W., 1953. The abundance of ^{18}O in atmospheric water ant water vapour. Tellus 5, 461–469.

Dansgaard, W., 1964. Stable isotopes in precipitation. Tellus 16, 436–468.

Dominik, J., Burrus, D., Vernet, J.-P., 1987. Transport of the environmental radionuclides in an alpine watershed. Earth Planet. Sci. Lett. 84, 165–180.

Epstein, S., Mayeda, T., 1953. Variation of ^{18}O content of waters from natural sources. Geochim. Cosmochim. Acta 4, 213–224.

Evrard, O., Némery, J., Gratiot, N., Duvert, C., Ayrault, S., Lefèvre, I., Poulenard, J., Prat, C., Bonté, P., Esteves, M., 2010. Sediment dynamics during the rainy season in tropical highland catchments of central Mexico using fallout radionuclides. Geomorphology 124, 42–54.

Gonfiantini, R., 1978. Standards for stable isotope measurements in natural compounds. Nature 271, 534–536.

González-Gómez, C., Azahra, M., López-Peñalver, J.J., Camacho-García, a, El Bardouni, T., Boukhal, H., 2006. Seasonal variability in ^{7}Be depositional fluxes at Granada, Spain. Appl. Radiat. Isot. 64, 228–34.

Gourdin, E., Evrard, O., Huon, S., Lefèvre, I., Ribolzi, O., Reyss, J.-L., Sengtaheuanghoung, O., Ayrault, S., Under review. Suspended sediment dynamics in a Southeast Asian mountainous catchment: combining river monitoring and fallout radionuclide analyses.

Harris, D.M., McDonnell, J.J., Rodhe, A., 1995. Hydrograph separation using continuous open system isotope mixing. Water Resour. Res. 31, 157–171.

Huh, C.-A., Su, C.-C., 2004. Distribution of fallout radionuclides (^{7}Be, ^{137}Cs, ^{210}Pb and ^{239,240}Pu) in soils of Taiwan. J. Environ. Radioact. 77, 87–100.

Huh, C.-A., Su, C.-C., Shiau, L.-J., 2006. Factors controlling temporal and spatial variations of atmospheric deposition of ^{7}Be and ^{210}Pb in northern Taiwan. J. Geophys. Res. 111, D16304.

Ingraham, N. and Taylor, B. E., 1991. Light stable Isotope systematics of large scale hydrologic regime in northern California and Nevada. Water Resour. Res., 27, 77-90.

Ioannidou, A., Papastefanou, C., 2006. Precipitation scavenging of ^{7}Be and ^{137}Cs radionuclides in air. J. Environ. Radioact. 85, 121–36.

Ishikawa, Y., Murakami, H., Sekine, T., Yoshihara, K., 1995. Precipitation scavenging studies of radionuclides in air using cosmogenic ^{7}Be. J. Environ. Radioact. 26, 19–36.

Iurian, A.-R., Toloza, A., Adu-Gyamfi, J., Cosma, C., 2013. Spatial distribution of ^{7}Be in soils of Lower Austria after heavy rains. J. Radioanal. Nucl. Chem. 298, 1857–1863.

Klaus, J., McDonnell, J.J., 2013. Hydrograph separation using stable isotopes: Review and evaluation. J. Hydrol. 505, 47–64.

Ladouche, B., Probst, A., Viville, D., Idir, S., Baqué, D., Loubet, M., Probst, J.-L., Bariac, T., 2001. Hydrograph separation using isotopic, chemical and hydrological approaches (Strengbach catchment , France). J. Hydrol. 242, 255–274.

Lal, D., Malhotra, P.K., Peters, B., 1958. On the production of radioisotopes in the atmosphere by cosmic radiation and their application to meteorology. J. Atmos. Terr. Phys. 12(4), 306–328.

Liu, G., Yang, M.Y., Warrington, D.N., Liu, P.L., Tian, J.L., 2011. Using beryllium-7 to monitor the relative proportions of interrill and rill erosion from loessal soil slopes in a single rainfall event. Earth Surf. Process. Landforms 36, 439–448.

Lozano, R.L., Hernández-Ceballos, M.A., Rodrigo, J.F., San Miguel, E.G., Casas-Ruiz, M., García-Tenorio, R., Bolívar, J.P., 2013. Mesoscale behavior of ^{7}Be and ^{210}Pb in superficial air along the Gulf of Cadiz (south of Iberian Peninsula). Atmos. Environ. 80, 75–84.

Mabit, L., Benmansour, M., Walling, D.E., 2008. Comparative advantages and limitations of the fallout radionuclides ^{137}Cs, $^{210}Pb_{ex}$ and ^{7}Be for assessing soil erosion and sedimentation. J. Environ. Radioact. 99, 1799–1807.

Matisoff, G., Bonniwell, E.C., Whiting, P.J., 2002. Radionuclides as indicators of sediment transport in agricultural watersheds that drain to Lake Erie. J. Environ. Qual. 31, 62–72.

Matisoff, G., Wilson, C.G., Whiting, P.J., 2005. The ^{7}Be/$^{210}Pb_{xs}$ ratio as an indicator of suspended sediment age or fraction new sediment in suspension. Earth Surf. Process. Landforms 30, 1191–1201.

McNeary, D., Baskaran, M., 2003. Depositional characteristics of ^{7}Be and ^{210}Pb in southeastern Michigan. J. Geophys. Res. 108, 4210.

Moore, H.E., Poet, S.E., Martell, E.A., 1973. ^{222}Rn, ^{210}Pb, ^{210}Bi, and ^{210}Po profiles and aerosol residence times versus altitude. J. Geophys. Res. 78, 7065–7075.

Morgan, R.P.C., 2009. Soil erosion and conservation. John Wiley & Sons.

Narazaki, Y., Fujitaka, K., Igarashi, S., Ishikawa, Y., Fujinami, N., 2003. Seasonal variation of ^{7}Be deposition in Japan. J. Radioanal. Nucl. Ch. 256(3), 489–496.

Olley, J., Burton, J., Smolders, K., Pantus, F., Pietsch, T., 2012. The application of fallout radionuclides to determine the dominant erosion process in water supply catchments of subtropical South-east Queensland, Australia. Hydrol. Process. 27(6), 885-895.

Olsen, C.R., Larsen, I.L., Lowry, P.D., Cutshall, N.H., Todd, J.F., Wong, G.T.F., Casey, W.H., 1985. Atmospheric fluxes and marsh-soil inventories of ^{7}Be and ^{210}Pb. J. Geophys. Res. Atmos. 90, 10487–10495.

Papastefanou, C., Ioannidou, A., 1995. Aerodynamic size association of ^{7}Be in ambient aerosols. J. Environ. Radioact. 26, 273–282.

Patin, J., Mouche, E., Ribolzi, O., Chaplot, V., Sengtahevanghoung, O., Latsachak, K.O., Soulileuth, B., Valentin, C., 2012. Analysis of runoff production at the plot scale during a long-term survey of a small agricultural catchment in Lao PDR. J. Hydrol. 426-427, 79–92.

Pham, M.K., Povinec, P.P., Nies, H., Betti, M., 2013. Dry and wet deposition of ^{7}Be, ^{210}Pb and ^{137}Cs in Monaco air during 1998-2010: seasonal variations of deposition fluxes. J. Environ. Radioact. 120, 45–57.

Pinto, V.M., Pires, L.F., Bacchi, O.O.S., Arthur, R.C.J., Bruno, I.P., Reichardt, K., 2013. Spatial variability of ^{7}Be fallout for erosion evaluation. Radiat. Phys. Chem. 83, 1–7.

Renfro, A.A., Cochran, J.K., Colle, B.A., 2013. Atmospheric fluxes of ^{7}Be and ^{210}Pb on monthly time-scales and during rainfall events at Stony Brook, New York (USA). J. Environ. Radioact. 116, 114–23.

Reyss, J.-L., Schmidt, S., Legeleux, F., Bonté, P., 1995. Large, low background well-type detectors for measurements of environmental radioactivity. Nuclear Instruments Methods Phys. Res. Sect. A Accel. Spectrometers, Detect. Assoc. Equip. 357, 391–397.

Ribolzi, O., Cuny, J., Sengsoulichanh, P., Mousquès, C., Soulileuth, B., Pierret, A., Huon, S., Sengtaheuanghoung, O., 2010. Land use and water quality along a Mekong tributary in northern Lao P.D.R. Environ. Manage. 47, 291–302.

Ribolzi, O., Cuny, J., Sengsoulichanh, P., Pierret, A., Thiebaux, J.P., Huon, S., Bourdon, E., Robain, H., Sengtaheuangoung, O., 2008. Assessment of water quality along a tributary of the Mekong River in a mountainous, mixed land-use environment of the Lao P.D.R. Lao J. Agric. For. 91–111.

Ribolzi, O., Vallès, V., Bariac, T., 1996. Comparison of hydrograph deconvolutions using residual alkalinity, chloride, and oxygen 18 as hydrochemical tracers. Water Resour. Res. 32, 1051–1059.

Saari, H.-K., Schmidt, S., Castaing, P., Blanc, G., Sautour, B., Masson, O., Cochran, J.K., 2010. The particulate $^{7}Be/^{210}Pb_{xs}$ and $^{234}Th/^{210}Pb_{xs}$ activity ratios as tracers for tidal-to-seasonal particle dynamics in the Gironde estuary (France): implications for the budget of particle-associated contaminants. Sci. Total Environ. 408, 4784–94.

Sidle, R.C., Ziegler, A.D., Negishi, J.N., Nik, A.R., Siew, R., Turkelboom, F., 2006. Erosion processes in steep terrain—Truths, myths, and uncertainties related to forest management in Southeast Asia. For. Ecol. Manage. 224, 199–225.

Su, C.-C., Huh, C.-A., 2006. Measurements of ^{7}Be and ^{210}Pb in cloudwaters: Toward a better understanding of aerosol transport and scavenging. Geophys. Res. Lett., 33, L04807, doi:10.1029/2005GL025042.

Talpos, S., Cuculeanu, V., 1997. A study of the vertical diffusion of ^{7}Be in the atmosphere. J. Environ. Radioact. 36, 93–106.

Taylor, A., Blake, W.H., Smith, H.G., Mabit, L., Keith-Roach, M.J., 2013. Assumptions and challenges in the use of fallout beryllium-7 as a soil and sediment tracer in river basins. Earth-Science Rev. 126, 85–95.

Turekian, K.K., Y., N., K., B.L., 1977. Geochemistry of atmospheric radon and radon products. Ann. Rev. Earth Planet. Sci. 5, 227–255.

Valentin, C., Agus, F., Alamban, R., Boosaner, A., Bricquet, J.-P., Chaplot, V., de Guzman, T., de Rouw, A., Janeau, J.-L., Orange, D., Phachomphonh, K., Podwojewski, P., Ribolzi, O., Silvera, N., Subagyono, K., Thiébaux, J.-P., Vadari, T., 2008. Runoff and sediment losses from 27 upland catchments in Southeast Asia: Impact of rapid land use changes and conservation practices. Agric. Ecosyst. Environ. 128, 225–238.

Vuille, M., Werner, M., Bradley, R.S., Keimig, F., 2005. Stable isotopes in precipitation in the Asian monsoon region. J. Geophys. Res. 110, 1–15.

Wallbrink, P., Murray, A., 1996. Distribution and variability of ^{7}Be in soils under different surface cover conditions and its potential for describing soil redistribution processes. Water Resour. Res. 32, 467–476.

Wallbrink, P.J., Murray, A.S., 1994. Fallout of ^{7}Be in South Eastern Australia. J. Environ. Radioact. 25, 213–228.

Walling, D.E., 2012. Beryllium-7: The Cinderella of fallout radionuclide sediment tracers? Hydrol. Process. 27, 830–844.

Wang, B., Clemens, S.C., Liu, P., 2003. Contrasting the Indian and East Asian monsoons: implications on geologic timescales. Mar. Geol. 201, 5–21.

Yamamoto, M., Sakaguchi, A., Sasaki, K., Hirose, K., Igarashi, Y., Kim, C.K., 2006. Seasonal and spatial variation of atmospheric ^{210}Pb and ^{7}Be deposition: features of the Japan Sea side of Japan. J. Environ. Radioact. 86, 110–31.

Figure captions

Fig. 1: Location of study site, contour lines, main stem and tributaries of the Houay Xon River. Location of daily cumulative and tipping bucket rain gauges. Long term mean monthly rainfall (1960-2013) in Luang Prabang (thin solid lines: standard deviation for each month; dashed lines: minimum and maximum values).

Fig. 2: Rainwater fractionated collection device at S10. left: pluviometer and collecting gutter; right: auto-capping 18L bottles connected to rainwater collection pipe.

Fig. 3: Rainfall intensity (mm min^{-1}) recorded at S1, CIM, S4 and S10 from June 2 to 4, 2013. Time lag between rainfall starting at S10 (vertical dashed line) and at other stations. Location of each pluviometer in the Houay Xon River catchment is displayed in Fig. 1.

Fig. 4: Rainfall intensity (mm min^{-1}) recorded at S10 from June 2 to 4, 2013, and corresponding rainwater samples oxygen stable isotopes ratio ($\delta^{18}O$, full circles), ^{7}Be (empty circles) and ^{210}Pb (squares) activities and ^{7}Be: ^{210}Pb ratio (triangles). Horizontal lines represent the collection period of each sample. Vertical error bars represent 1σ uncertainty.

Fig. 5: Rainwater samples ^{7}Be and ^{210}Pb activities (a-b), cumulative depositions (c-d) and activity ratios (e-f) versus cumulative rainfall recorded at S10 on June 2 and 4, 2013. Horizontal lines represent the collection period of each sample. Vertical error bars represent 1σ uncertainty.

Fig. 6: Temporal variability of radionuclide deposition storm by storm at S10 (from June 2 to 4, 2013): cumulative rainfall (mm), cumulative ^{7}Be and ^{210}Pb deposition (Bq m^{-2}) and ^{7}Be: ^{210}Pb ratio. Error bars represent 1σ uncertainty.

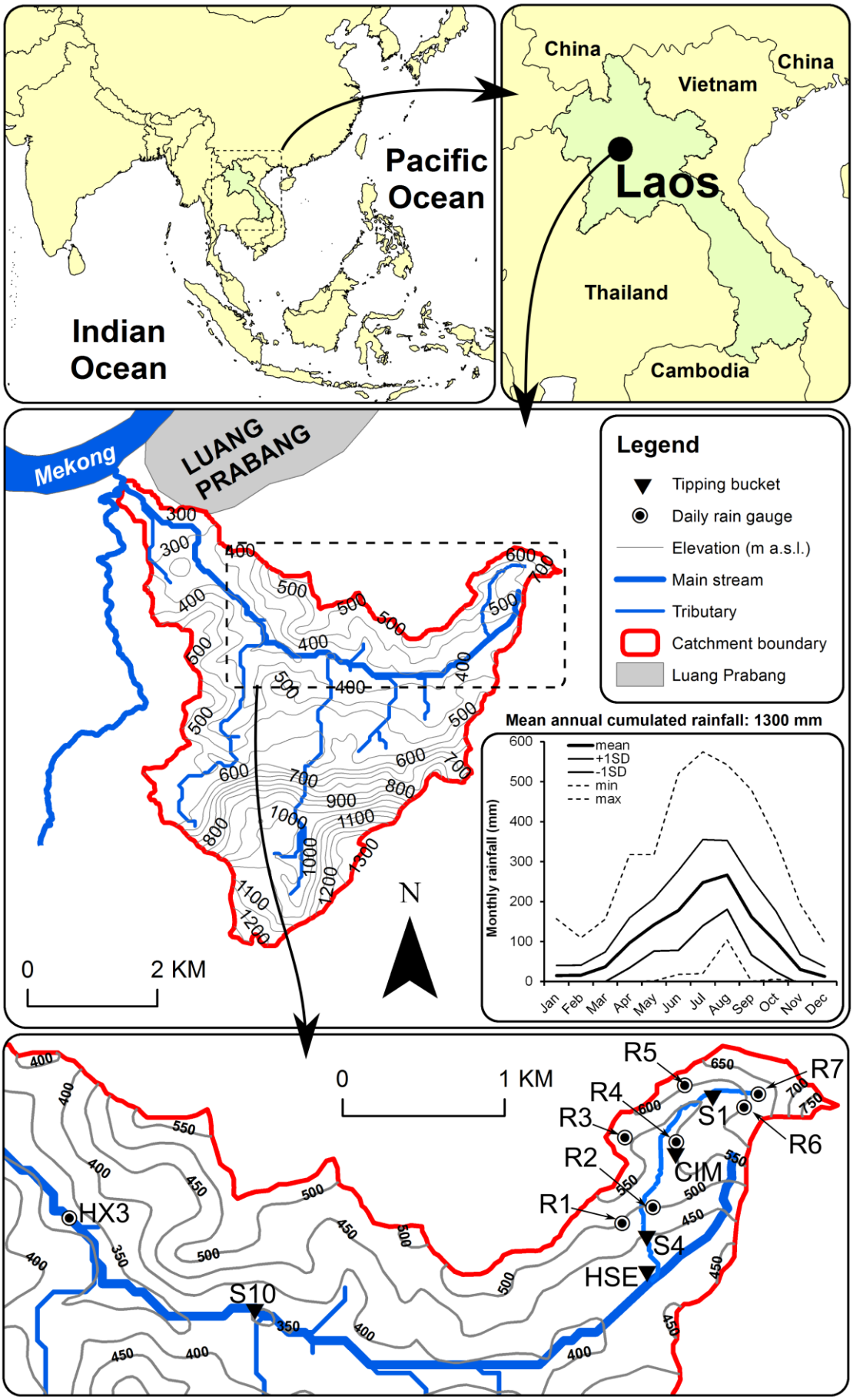

Fig. 1: Location of study site, contour lines, main stem and tributaries of the Houay Xon River catchment. Location of daily cumulative and tipping bucket rain gauges. Long term mean monthly rainfall (1960-2013) in Luang Prabang (thin solid lines: standard deviation for each month; dashed lines: minimum and maximum values recorded).

Fig. 2: Rainwater fractionated collection device at S10. left: pluviometer and collecting gutter; right: auto-capping 18L bottles connected to rainwater collection pipe.

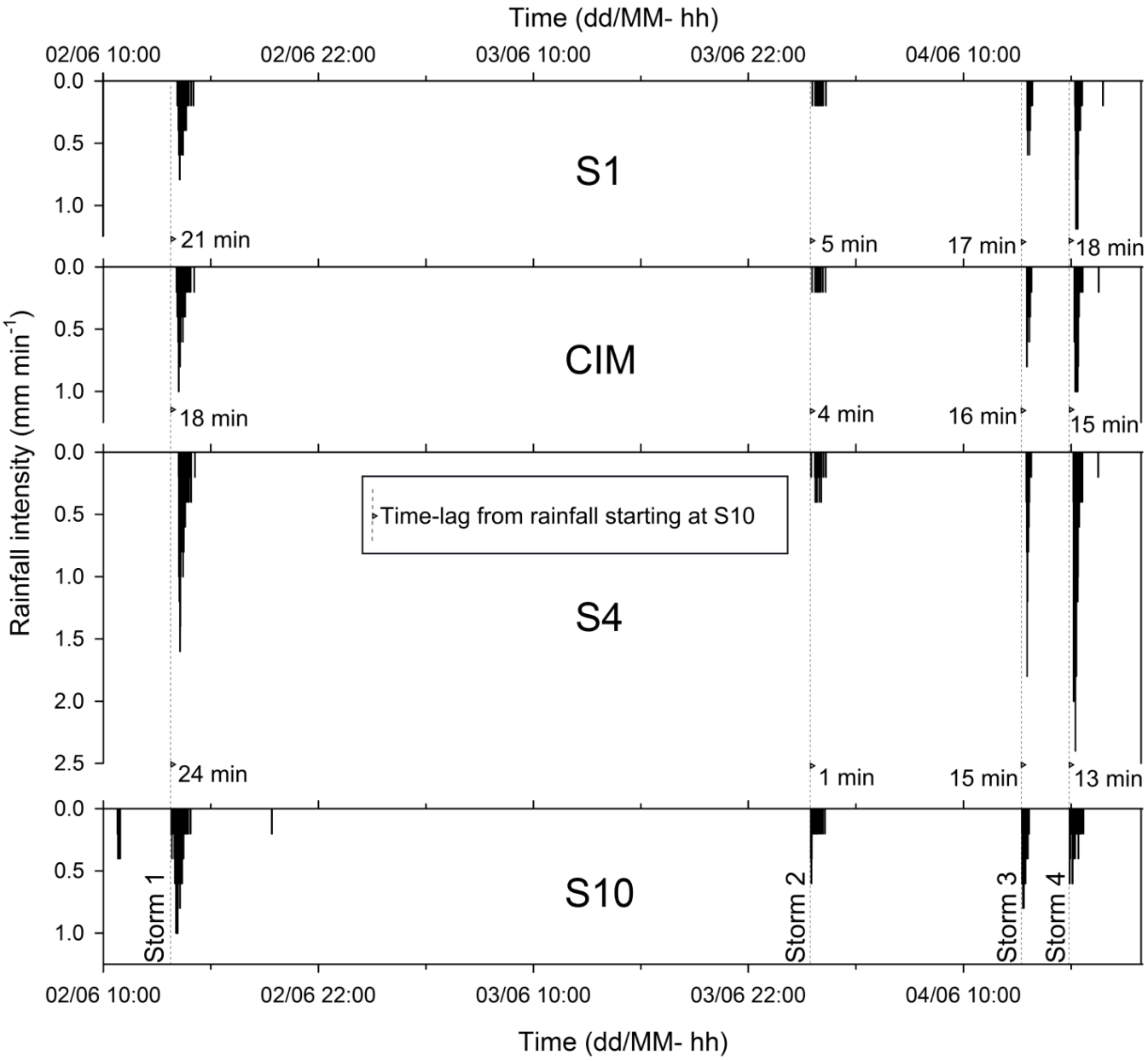

Fig. 3: Rainfall intensity (mm min^{-1}) recorded at S1, CIM, S4 and S10 from June 2 to June 4, 2013. Time-lag between rainfall starting at S10 and at other stations. Location of each pluviometer in the Houay Xon River catchment is provided on Fig. 1.

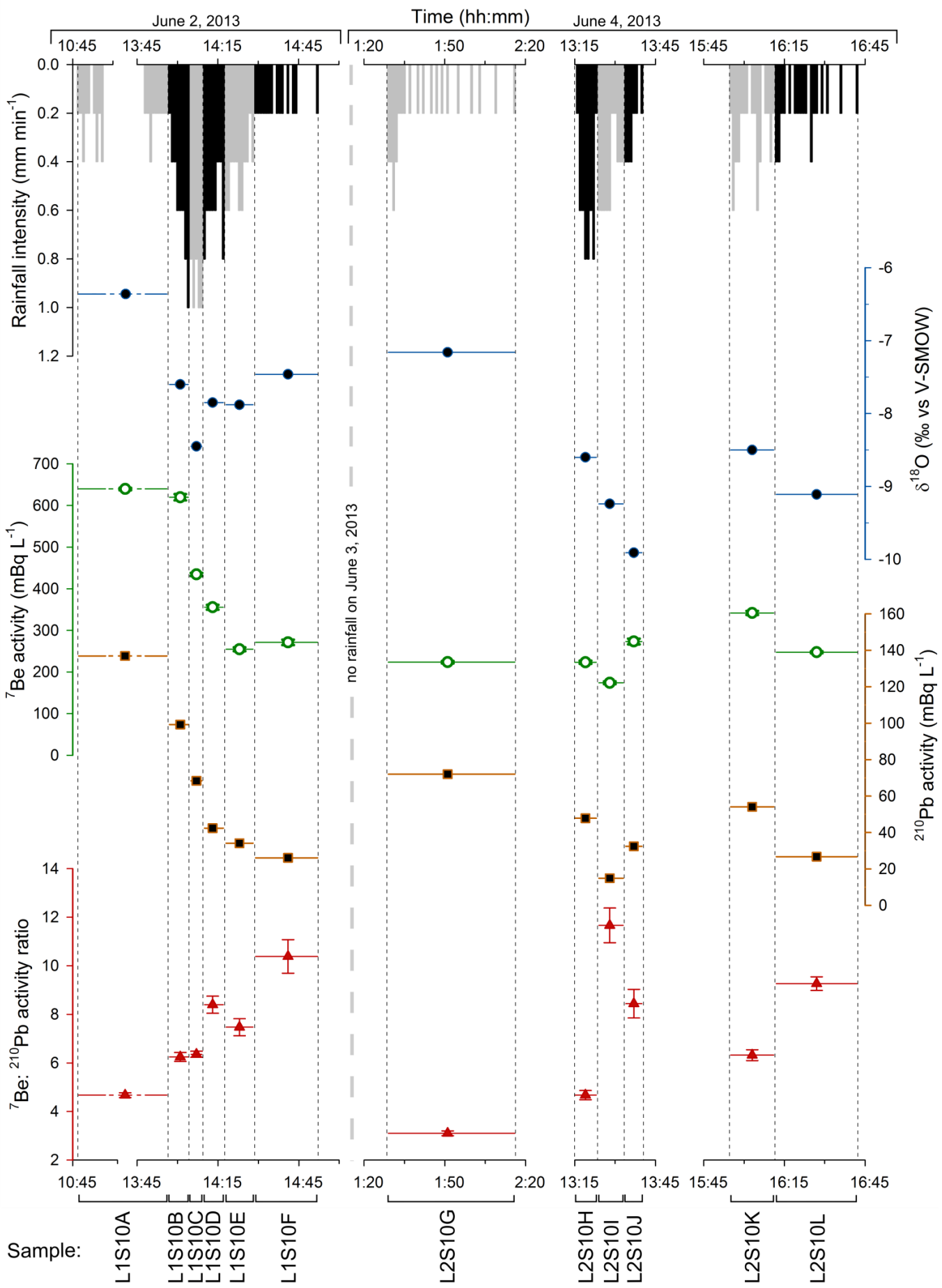

Fig. 4: Rainfall intensity (mm min^{-1}) recorded at S10 from June 2 to 4, 2013 and corresponding rainwater samples oxygen isotopic ratio ($\delta^{18}O$, full circles), ^{7}Be (empty circles) and ^{210}Pb (squares) activities and ^{7}Be: ^{210}Pb ratio (triangles). Horizontal lines represent the collection period of each sample. Error bars

represent 1σ uncertainty.

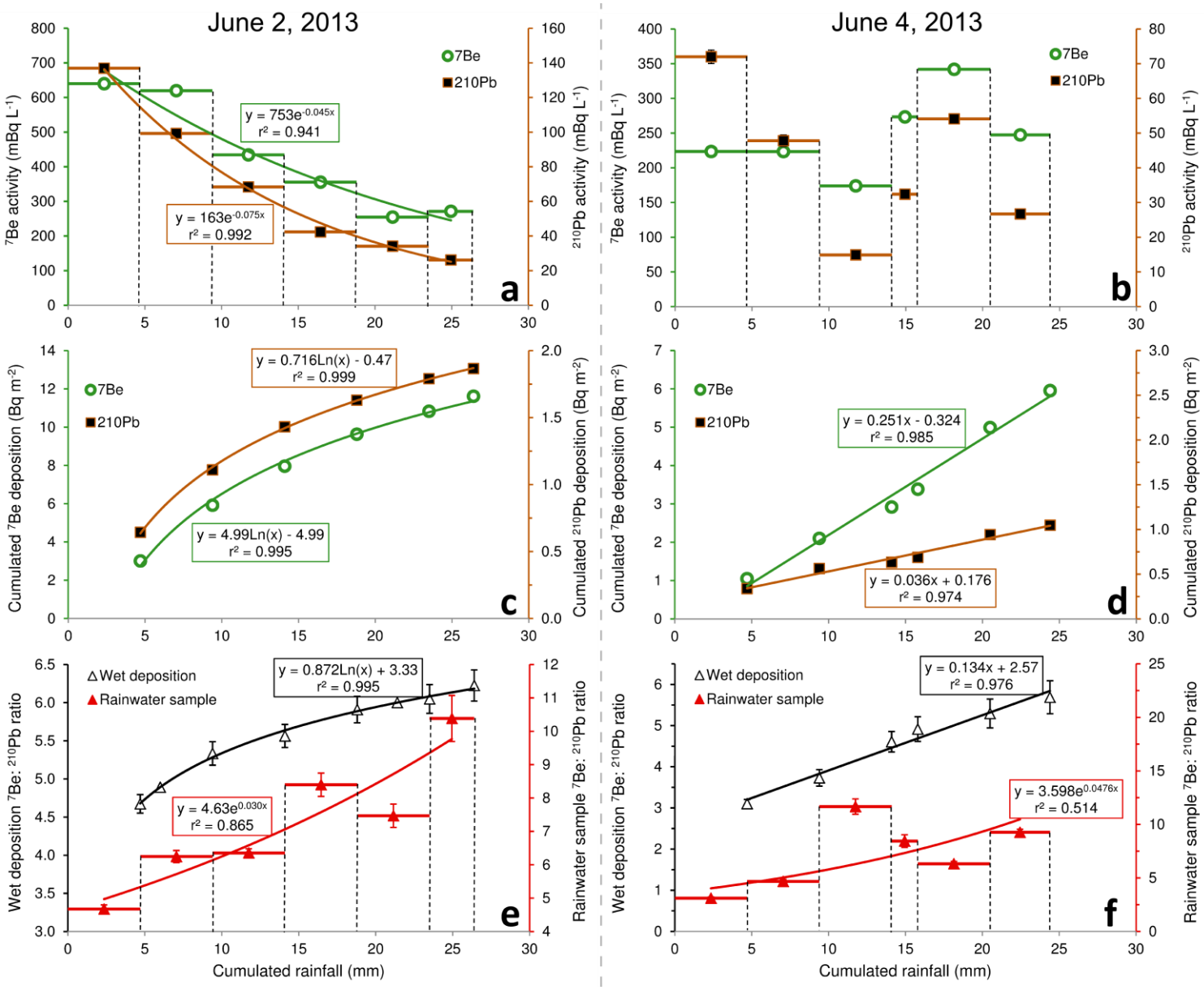

Fig. 5: Rainwater samples ^{7}Be and ^{210}Pb activities (a-b), cumulated depositions (c-d) and activity ratios (e-f) versus cumulated rainfall recorded at S10 on June 2 and 4, 2013. Horizontal lines represent the collection period of each sample. Vertical error bars represent 1σ uncertainty.

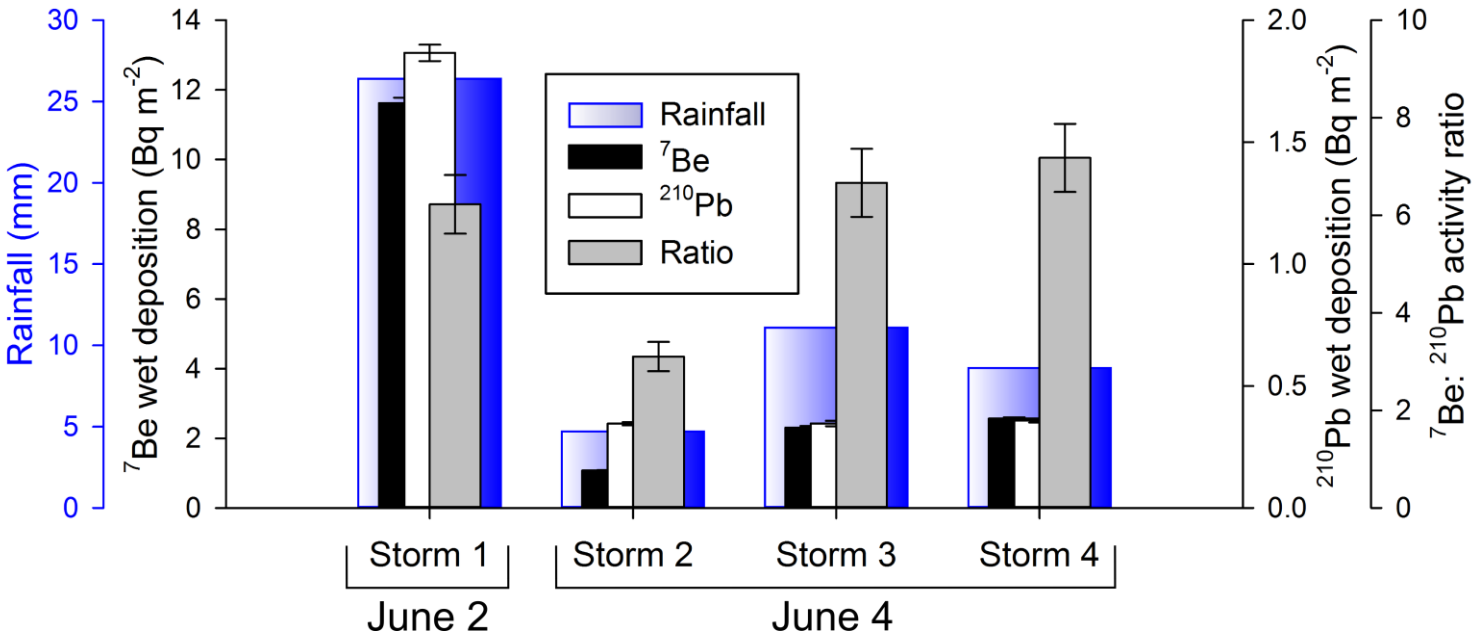

Fig. 6: Temporal variability of radionuclide deposition storm by storm at S10 (from June 2 to 4): cumulated rainfall (mm), cumulated ^{7}Be and ^{210}Pb deposition (Bq m^{-2}) and ^{7}Be: ^{210}Pb ratio. Error bars represent 1σ uncertainty.

Table 1. Characteristics of rainfall monitoring and sampling stations in the Houay Xon catchment.

Station	Collecting area (m^2)	Number of samples June 2 / June 4	Type of rainwater sampler	Rainfall intensity measurement	
				Device	Frequency
S1	0.04	-	-	Tipping-bucket rain gauge	1 min (0.2 mm increments)
CIM	0.04	-	-	Tipping-bucket rain gauge	1 min (0.2 mm increments)
S4	0.14	1 / 1	cumulative	Tipping-bucket rain gauge	1 min (0.2 mm increments)
HSE	0.04	-	-	Tipping-bucket rain gauge	30 min
S10	4	6 / 6	fractionated *	Tipping-bucket rain gauge	1 min (0.2 mm increments)
HX3	0.14	1 / -	cumulative	Bucket	1 day

- : no sampling * : max 4.7 mm / sample

Table 2. Elevation and cumulated precipitation on June 2 and June 4, 2013 at the 13 rain gauging stations installed across Houay Xon River catchment (increasing elevation from left to right).

Parameter		(unit)	Stations											
			HX3	S10	HSE	S4	R2	R1	CIM	R4	R3	S1	R5	R6	R7
Elevation		(m a.s.l.)	330	350	410	450	509	510	536	563	567	570	586	604	614
Precipitation	June 2	(mm d^{-1})	27.1	26.4	20.9	20.6	20.2	20.4	14.6	13.9	17.0	12.5	14.4	12.1	10.8
	June 4	(mm d^{-1})	-	24.4	32.4	39.8	29.2	31.4	23.8	28.0	25.8	20.6	14.2	17.9	18.6
	Total	(mm)	-	50.8	53.3	60.4	49.4	51.8	38.4	41.9	42.8	33.1	28.6	30.0	29.4

- : no data

Table 3. Spatial variability of cumulated radionuclide activity (mBq L^{-1}) and wet deposition (Bq m^{-2}), resulting ^{7}Be: ^{210}Pb ratio and rainwater $\delta^{18}O$ on June 2 and June 4, 2013, and cumulated over all monitoring period (Total = June2 + June4) across Houay Xon catchment.

Date	Station	^{7}Be		^{210}Pb		^{7}Be: ^{210}Pb ratio	$\delta^{18}O$
		(mBq L^{-1})	(Bq m^{-2})	(mBq L^{-1})	(Bq m^{-2})		(‰)
June 2	S4	1130 ± 25	23.3 ± 0.5	189 ± 5	3.9 ± 0.11	6.0 ± 0.3	-7.6
	S10	440 ± 4*	11.6 ± 1.0*	71 ± 0.8*	1.9 ± 0.1*	6.2 ± 0.3*	-7.6*
	HX3	1718 ± 71	46.6 ± 1.9	263 ± 12	7.1 ± 0.3	6.5 ± 0.6	-7.3
June 4	S4	848 ± 54	33.8 ± 2.1	94 ± 10	3.8 ± 0.4	9.0 ± 1.5	-6.7
	S10	244 ± 3*	6.0 ± 0.1*	43 ± 0.8*	1.1 ± 0.1*	5.7 ± 0.2*	-8.6*
Total	S4	-	57.1 ± 6.3	-	7.2 ± 1.1	7.9 ± 2.1	-
	S10	-	17.6 ± 0.5	-	2.9 ± 0.2	6.1 ± 0.6	-

- : no data; * : total daily wet deposition (calculated from data displayed in Appendix)

Table 4. Comparison of ^{7}Be and ^{210}Pb wet deposition and spatial coefficient of variation (CV) during individual storms and for monthly deposition from literature data

Reference	Location	Latitude	Study spatial scale		Study duration	N° of storm sampled	Rainfall depth per storm (mm)	Daily wet deposition (Bq m^{-2} d^{-1})			Spatial CV (%)**		
			Size/ distance	N° of station				^{7}Be	^{210}Pb	Ratio	^{7}Be	^{210}Pb	Ratio
Renfro et al., 2013	New York (USA)	40.9°N	-	1	19 mo.	4	8 - 40	40.1 ± 3.3 - 123.3 ± 5.0	0.3 ± 0.1 - 0.4 ± 0.1	132 ± 41 - 286 ± 71	-	-	-
Conaway et al., 2013	California (USA)	37°N	5 km	2	10 mo.	20	7 - 140	12 ± 2 - 188 ± 3	-	-	13 - 49	-	-
Huh et al., 2006	Taiwan	25°N	~20 km	2	9 y.	418	< 420	<300	<50	<19	75	69	29
This study	Northern Laos	19.9°N	3 km	4	3 d.	4	4 - 40	6.0 ± 0.1 - 46.6 ± 1.9	1.1 ± 0.1 - 7.1 ± 0.3	5.7 ± 0.2 - 9.0 ± 1.5	65 - 70	61 - 62	4 - 22
Pinto et al., 2013	Piracicaba (Brazil)	22.7°S	300 m^{2}	12	16 mo.	5	4.5 - 21	2.1 ± 1.2 - 12.8 ± 3.8	-	-	20 - 64	-	-
Wallbrink and Murray, 1994	Southern Australia	35°S	-	1	17 mo.	83	0.1 - 160	<1 - 123	-	-	-	-	-
Renfro et al., 2013	New York (USA)	40.9°N	-	1	*19 mo.*	-	*36 - 190*	*67 ± 2 - 385 ± 8*	*6.7 ± 0.5 - 16.7 ± 0.9*	*10.0 ± 0.8 - 28.1 ± 0.9*	-	-	-
Yamamoto et al., 2006	Japan and Korea	33.6 - 45.4°N	1600 km	*1* - **12**	*12 y.* - **2 y.**	-	*4 - 450*	*5 - 1650*	*2 - 245*	*4 - 17*	**47**	**55 - 63**	**22**
Lozano et al. 2013	Southern Spain	36 - 37°N	100 km	2	*2.5 y.*	-	*5 - 230*	*1.1 ± 0.2 - 204 ± 7*	*0.23 ± 0.15 - 14.9 ± 0.5*	*4.5 ± 3.0 - 30.6 ± 2.2*	*14 - 99*	*2 - 69*	*2 - 95*
Huh and Su, 2004	Taiwan	25°N	400 km	152	5 y.	-	-	310 - 5290 *	3300 - 81700 *	0.1 - 0.5 *	10 - 85 *	4 - 80 *	-
Wallbrink and Murray, 1996 *	Southern Australia	35°S	20 m	3	20 mo.	-	-	85 ± 15 - 450 ± 40 *	-	-	5 - 25 *	-	-

- = no data *italic :* monthly deposition values **bold** : annual deposition values * : soil inventory values ** : CV = Std.Dev. ÷ Mean ∗ 100

Appendix. Sequential intra-storm sampling results: ^{7}Be and ^{210}Pb activities (mBq L^{-1}) and atmospheric fluxes (Bq m^{-2}) on June 2 and June 4, 2013 at S10 station. T: start and end time of sampling. dT: duration of sampling. Rain: cumulated rainfall associated with each sample. Ratio: ^{7}Be: ^{210}Pb activity ratio. Oxygen isotopic ratio ($\delta^{18}O$). Uncertainties are given as 1σ counting statistics.

Date	Sample	T		dT	P	^{7}Be		^{210}Pb		Ratio	$\delta^{18}O$
		(hh:mm)		(min)	(mm)	(mBq L^{-1})	(Bq m^{-2})	(mBq L^{-1})	(Bq m^{-2})	(Bq/Bq)	(‰)
June 2 2013	L1S10A	10:46	13:56	10+10	4.7	640 ± 8	3.0 ± 0.04	137 ± 1.9	0.64 ± 0.009	4.7 ± 0.1	-6.4
	L1S10B	13:56	14:04	8	4.7	620 ± 8	2.9 ± 0.04	99 ± 1.7	0.47 ± 0.008	6.3 ± 0.2	-7.6
	L1S10C	14:04	14:09	5	4.7	434 ± 4	2.0 ± 0.02	68 ± 0.8	0.32 ± 0.004	6.4 ± 0.1	-8.5
	L1S10D	14:09	14:17	8	4.7	356 ± 6	1.7 ± 0.03	42 ± 1.1	0.20 ± 0.005	8.4 ± 0.4	-7.9
	L1S10E	14:17	14:28	11	4.7	255 ± 5	1.2 ± 0.02	34 ± 1.0	0.16 ± 0.005	7.5 ± 0.4	-7.9
	L1S10F	14:28	14:52	24	2.9	271 ± 7	0.8 ± 0.02	26 ± 1.1	0.08 ± 0.003	10.4 ± 0.7	-7.5
June 4 2013	L2S10G	01:28	02:16	48	4.7	224 ± 3	1.1 ± 0.01	72 ± 1.4	0.34 ± 0.007	3.1 ± 0.1	-7.2
	L2S10H	13:15	13:23	8	4.7	223 ± 4	1.0 ± 0.02	48 ± 1.1	0.22 ± 0.005	4.7 ± 0.2	-8.6
	L2S10I	13:23	13:33	10	4.7	174 ± 3	0.8 ± 0.02	15 ± 0.6	0.07 ± 0.003	11.7 ± 0.7	-9.2
	L2S10J	13:33	13:40	7	1.7	273 ± 7	0.5 ± 0.01	32 ± 1.5	0.06 ± 0.002	8.4 ± 0.6	-9.9
	L2S10K	15:54	16:11	17	4.7	342 ± 5	1.6 ± 0.02	54 ± 1.2	0.25 ± 0.005	6.3 ± 0.2	-8.5
	L2S10L	16:11	16:42	36	3.9	247 ± 3	1.0 ± 0.01	27 ± 0.5	0.10 ± 0.002	9.3 ± 0.3	-9.1